1D Josephson quantum interference grids: diffraction patterns and dynamics

M Lucci[1], D Badoni[1], V Corato[1,4], V Merlo[1], I Ottaviani[1], G Salina[1], M Cirillo[1,5], A V Ustinov[2] and D Winkler[3]

[1] Dipartimento di Fisica and MINAS Lab, Università di Roma Tor Vergata, 00133 Roma, Italy and INFN sezione 'Tor Vergata', via della Ricerca Scientifica, 00133 Roma, Italy
[2] Physikalisches Institut, Karlsruhe Institute of Technology, D-76128 Karlsruhe, Germany and National University of Science and Technology MISIS, Leninsky prosp. 4, Moscow, 119049, Russia
[3] Department of Microtechnology and Nanoscience—MC2, Chalmers University of Technology, SE-412 96 Göteborg, Sweden

Abstract

We investigate the magnetic response of transmission lines with embedded Josephson junctions and thus generating a 1D underdamped array. The measured multi-junction interference patterns are compared with the theoretical predictions for Josephson supercurrent modulations when an external magnetic field couples both to the inter-junction loops and to the junctions themselves. The results provide a striking example of the analogy between Josephson phase modulation and 1D optical diffraction grid. The Fiske resonances in the current-voltage characteristics with voltage spacing $\Phi_0\left(\frac{\bar{c}}{2L}\right)$, where L is the total physical length of the array, Φ_0 the magnetic flux quantum and $\bar{c}$ the speed of light in the transmission line, demonstrate that the discrete line supports stable dynamic patterns generated by the ac Josephson effect interacting with the cavity modes of the line.

Keywords: superconductivity, Josephson effect, arrays of Josephson junctions

(Some figures may appear in colour only in the online journal)

Arrays of Josephson junctions have attracted attention in the past decades due to their remarkable versatility for modelling, in one [1] and two spatial dimensions [2], of ensembles of solid-state nonlinear oscillators. Statistical mechanics [3] and generation of electromagnetic radiation in the terahertz gap of the electromagnetic wave spectrum motivated the fundamental and applied physics community towards the investigation of array properties. Recently, the search for new computational concepts [4–6] tending to lower the power dissipation in digital circuits, has focused back the attention to 1D arrays of Josephson junctions. These computational ideas are heavily based on flux-quanta motion in 1D underdamped arrays under the condition in which the inductances connecting the junctions are very low, a physical configuration that we identify as 'strong coupling' between the junctions of the arrays. Here, we undertake a systematic investigation of this kind of arrays in order to clarify their internal dynamics and provide input for the design and margins of the physical parameters of the devices operating in this regime. Our recent spectroscopic microwave study [7] of parallel arrays has revealed intriguing features concerning the dynamics of magnetic flux quanta in these structures. We herein investigate the modulation of Josephson supercurrent and Fiske singularities induced by an external magnetic field in arrays of junctions of finite dimensions and compare the obtained results with theoretical predictions. As far as the supercurrent modulations are concerned we show that a functional dependence [8] which extended results published by Miller *et al* [9] can provide good account of the experiments for the case of uniform arrays (junctions of the arrays having the same size, critical current and mutual spacing).

[4] Unità Tecnica Fusione-ENEA C.R. Frascati, via E. Fermi 45, 00044 Frascati (Roma), Italy.
[5] Also at CNR-SPIN Institute, Via Giovanni Paolo II, 84084 Fisciano (SA).
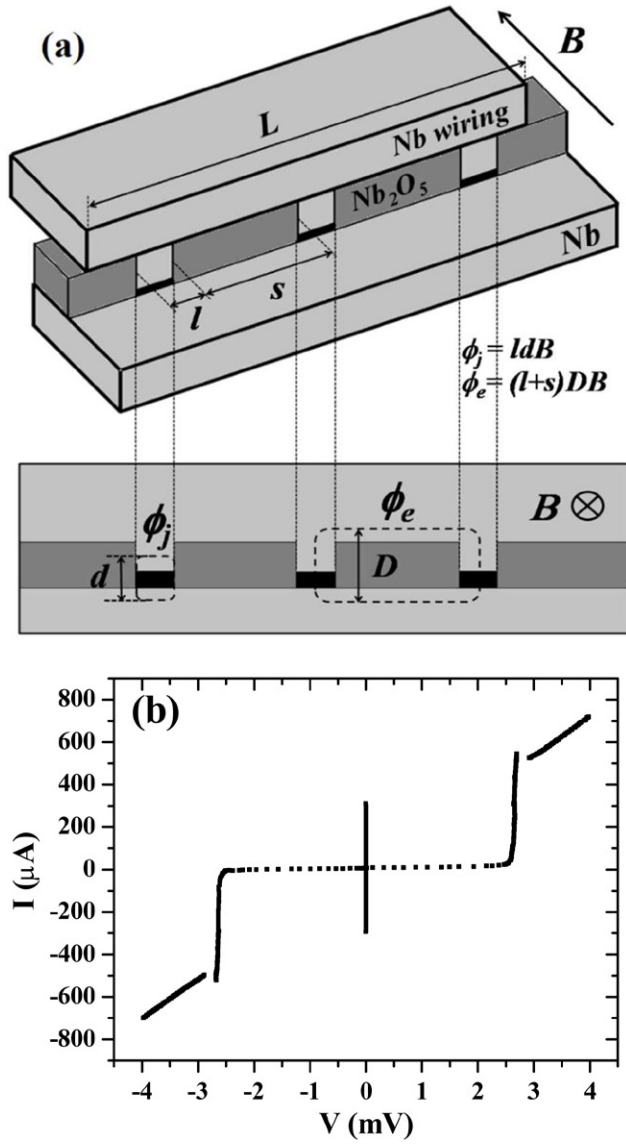
Figure 1. (a) Sketch of a three-junction interferometer indicating the magnetic fluxes threading the junctions and the loops connecting them. The locations of the tunnel junctions are indicated by the black-coloured regions. The direction of the applied external magnetic field, indicated by the arrow in the figure, is in the plane of the junctions. (b) A typical current-voltage characteristic of our samples, here for a three-junction interferometer.

Figure 1 shows a sketch of the samples that we have used for the experiments. We study Josephson junctions connected in parallel by the small inductances generated by niobium superconducting electrodes; the technological procedure for obtaining the tunnel junctions is based on the Nb trilayer process (Nb/AlOx/Nb) for window-type junctions in which extra-isolation between electrodes is provided by the anodic oxide (Nb$_2$O$_5$) [10]. The thickness of the Nb films constituting a junction was 120 nm for the base electrode and 230 for top-contact electrode. We shall comment later on the thickness of the oxide layer, which is of the order of few nanometers. Overall, the samples are transmission lines generated by the superconducting electrodes in which the Josephson junctions represent regions with increased local capacitance and are also commonly referred to as Josephson transmission lines

(JTLs); d and D represent the magnetic penetration depths in the regions where junctions are present (d) or not (D). Given I_{C0} (the maximum Josephson current in zero applied magnetic field), R_n (the normal-state tunnelling resistance), R_{sg} (the subgap resistance), the junctions that we used for the experiments had excellent properties with $I_{C0}R_n \approx 1.6$ mV and $V_N = I_{C0} R_{sg}$ up to 60 mV (with R_{sg} measured at 2 mV). From the magnetic field diffraction patterns of test junctions we calculated that the London penetration depth of our samples is 90 nm and therefore $d = 180$ nm (neglecting the few nanometers of oxide thickness). We estimate the error on the London penetration depth to be below 5%.

In figure 1(b), we show the current-voltage (*IV*) characteristics of a three junction interferometer. The major geometrical dimensions of our samples are indicated in figure 1(a). A model for the magnetic field dependence of the critical current of linear arrays composed of Josephson junctions (also called SQUIGs, namely Superconducting Quantum Interference Grids) was published by Miller *et al* [9]. For convenience, we report here their equation for the critical current pattern (note that typos were present in the version published in the journal, equation (2) of [9]. The correct equation should be

$$I_c(\phi_e) = I_{C0} \left| \frac{\sin\left[(N+1)\frac{\pi\phi_e}{\Phi_0}\right]}{\sin\left(\frac{\pi\phi_e}{\Phi_0}\right)} \right| \qquad (1)$$

In this equation N is the number of loops of the array (by consequence, $N + 1$ is the number of junctions), $\Phi_0 = 2.07 \times 10^{-15}$ *Wb* is the magnetic flux quantum and I_{C0} is the maximum critical current of a single junction of the array; ϕ_e is the flux of the magnetic induction vector (*B*) threading the loops between the junctions, which has the value $BD(l + s)$ in terms of the notations introduced in figure 1. We note that, in the limit $N = 1$, namely considering the case of a single interferometer with two ($N + 1 = 2$) junctions, equation (1) becomes

$$I_c(\phi_e) = 2I_{C0} \left| \cos\left(\frac{\pi\phi_e}{\Phi_0}\right) \right| \qquad (2)$$

which is the well-known functional dependence for a two-junction interferometer [11]. One can see that on the right hand side the dependence upon $\phi_j = Bdl$ (the flux threading the *j*-th junction) does not appear because equation (1) was derived in the limit of 'point-like' junctions meaning that the contribution of the flux penetrating the junctions themselves is neglected. However, when the size of the junctions forming the arrays is different from zero (as it is for a point-like junction), equation (1) takes another functional dependence which reads [8]

$$I_c(\phi_e, \phi_j) = I_{C0} \left| \frac{\sin\left[(N+1)\frac{\pi\phi_e}{\Phi_0}\right]}{\sin\left(\frac{\pi\phi_e}{\Phi_0}\right)} \right| \left| \frac{\sin\left(\frac{\pi\phi_j}{\Phi_0}\right)}{\left(\frac{\pi\phi_j}{\Phi_0}\right)} \right| \qquad (3)$$

In terms of figure 1, ϕ_j is the magnetic flux penetrating the *j*-th junction having the magnetic field penetration depth d. In the limit ϕ_j tending to zero (no flux through the junctions)

J. Phys. D: Appl. Phys. **49** (2016) 065303

M Lucci *et al*

the second term on the right hand side gives unity and equation (3) is reduced to equation (1). For the purposes of the present paper, in which we have arrays made of junctions of the same size separated by equal distances and the dimensions of the junctions not negligible with respect to those of the loops, we shall attempt to use equation (3) for interpreting the data. We have worked out, similarly to other groups [12], generalization of this equation which can be applied to non-uniform arrays made of junctions with different supercurrents and uneven spacing, but these results shall be dealt in a future publication. It is worth noting that, when deriving equation (3), the normalized flux generated by the Josephson current through the inductor (l_0) connecting the junctions, namely $l_0 I_{C0}/\Phi_0$, is considered negligible and set to zero. In our case, this normalized parameter is in the range (0.01–0.15) and thus the approximation is reasonable. The theoretical model presented in [8], however, also reported on a perturbation analysis calculating deviations from equation (3) due to a small, but non-zero Josephson current flux. We shall also analyze the predictions of this model in connection with our results. It is worth pointing out that equation (3) is analogous to the well-known dependence of the light intensity on a diffraction grating when the size of the slits is taken into account [13].

In figure 2(a), we show the modulation of the maximum Josephson supercurrent of a two junction interferometer which is made of (14 μm $\times$ 14 μm) square junctions separated by a 2 μm gap. The curve through the data is obtained from equation (3) by normalizing the current to the maximum Josephson current of the interferometer ($2I_{C0}$ in this case). One can see that the behaviour is much like the Fraunhofer pattern of a single junction. However, in the remainder of figure 2, we show a sequence of the effect on the interferometer modulations due to the increased separation s between the junctions. In particular, in figure 2(b) the spacing between the junctions is 10 μm while in figure 2(c) it is 30 μm; the areas of the junctions are identical to those of figure 1(a). We can clearly see that increasing the spacing between the junctions (and therefore the flux threading the loops) the 'interferometric' character of the patterns becomes increasingly evident. All the curves through the data in figure 2 are obtained from equation (3) using d and D as fitting parameters. The magnetic fluxes in this equation are obtained just by multiplying the external magnetic field by the geometrical parameters shown in figure 1. The value of the magnetic penetration depth of the junctions corresponding to the best fit to the data of figure 2 is $d = 180$ nm. As far as D is concerned, the value that gave the best fit to the data was 300 nm which is consistent with our expectation from the fabrication procedure. Given the shape and the critical current density ($j_c = 110$ A cm^{-2}) of our samples and $\mu_0 = 4\pi \times 10^{-7}$ H m^{-1} the 'minimal' Josephson penetration depth $\lambda_j = \sqrt{\frac{\Phi_0}{2\pi\mu_0 d j_c}}$ our samples is 36 μm while we estimate that the effective Josephson penetration depth λ_{jeff} [14] of our samples lying in the range (35 μm–60 μm). In any case the size of our junctions is such that the junction themselves can be seen as 'small' junctions because their physical dimensions are smaller than the Josephson penetration depth.
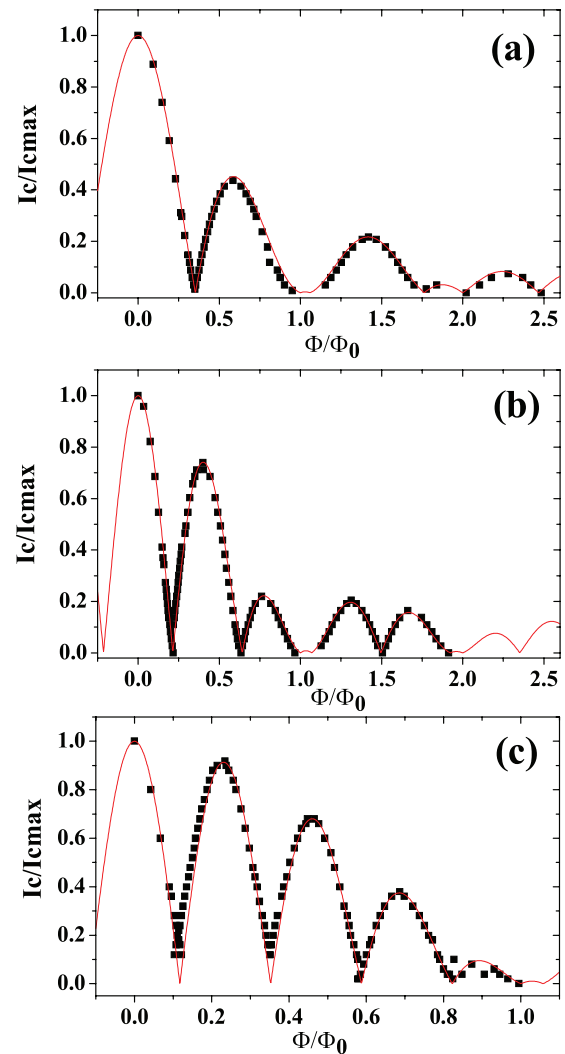
Two junctions interferometers

Figure 2. Magnetic field pattern for a two-junction interferometer with a given area (14 μm $\times$ 14 μm) of the junctions and increasing their separation distance. In (a), (b), and (c) the distance (between the sides of the junctions, s in terms of figure 1(a) is, respectively 2 μm, 10 μm, and 30 μm. Increasing the distance between the junctions the 'interferometric' part due to the connecting loops increases its relevance over the single-junction Fraunhofer-like contribution. The curves fitting the data are obtained from equation (3).

Comparing our figure 2(c) with figure 5 of [8] we realize that our data show results consistent with the predictions of the perturbative approach. Notice, when comparing the vertical scales of the figures that the factor *2* is just due to a different choice of the maximum current value; in our case 1 corresponds to the maximum current flowing through both the junctions, i. e. $2I_{C0}$. We see in particular in our figure 2(c) that the Josephson current does not modulate to zero: this effect must be attributed to the fact that we cannot neglect here the effect of the normalized Josephson flux which we estimate to be 0.15 in this case. For the above mentioned figure of [8] we see that the perturbative correction due to a non-zero
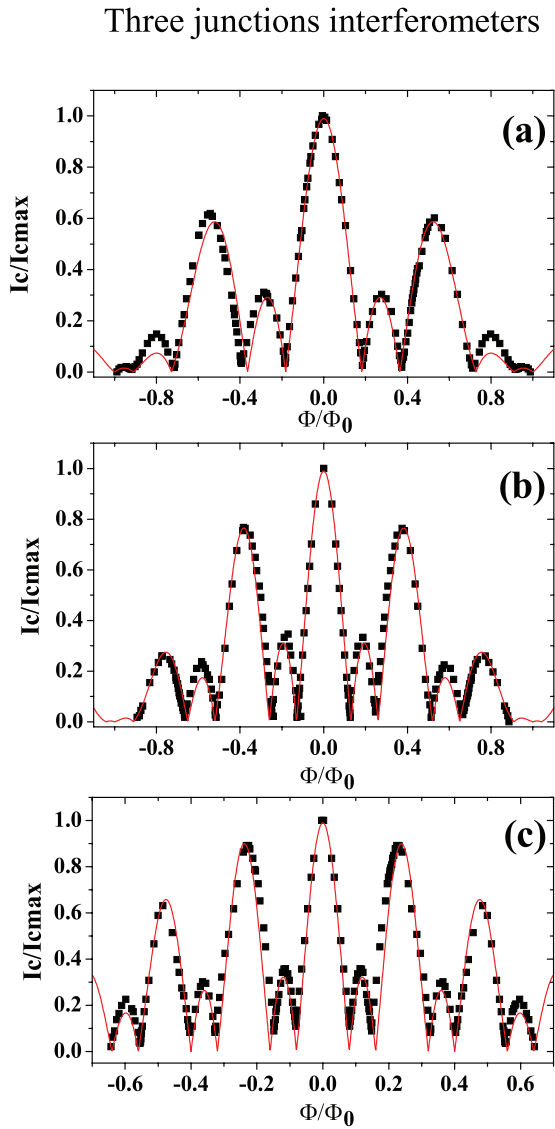
Three junctions interferometers
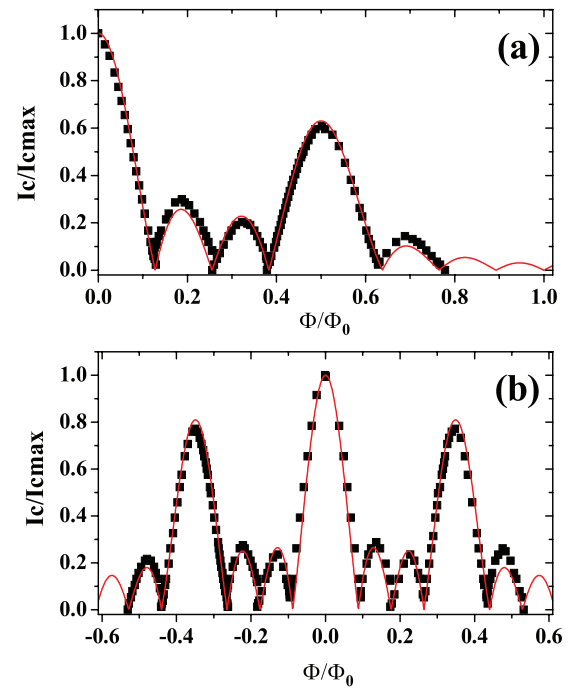

Four junctions interferometers

Figure 4. The modulation of the Josephson critical current of an array made of four junctions in parallel. The areas of the junctions are the same as in figures 2 and 3 while distances are 5 μm and 10 μm, respectively, for (a) and (b).

Figure 3. The data analogous to that shown in figure 2, but for a three-junction interferometer. The areas of the junctions are 14 μm × 14 μm), as in figure 2, while the distances are, 5 μm, 10 μm, and 20 μm, respectively, for (a), (b), and (c). Here, as in figure 2, the fit is to equation (3). Note that in (c) the data points do not reach zero due to the increased contribution of the flux through the loops of the Josephson currents, which are neglected when deriving equation (3).

Josephson flux generates a minimum in the modulations of the current in the same range observed in our experiments.

Figure 3 shows a sequence similar to the one reported in figure 2, but here for a three-junction arrays. The size of the junctions is as in figure 2 and the separation between the junctions is 5 μm, 10 μm, and 20 μm, respectively, for (a), (b), and (c). While increasing the separation between the junctions the interference effect between them increases as well. A double-period modulation indicates critical current amplitude oscillations that take place over different magnetic field periods. The curves through the data are obtained from equation (3). We can conclude that equation (3) provides excellent account for the experimental results. One can see in figure 3(c), as for figure 2(c), that when the distance between the junctions

increases the experimental critical current modulation does not attain values close to zero, as in the other cases, while the theoretical curve does go to zero. As before, this effect is a consequence of the fact that the flux due to the Josephson currents cannot be neglected, meaning that equation (3) fails explaining the data and a more complex model and/or numerical simulations should be considered [8]. For figure 3(c) we estimate a normalized Josephson flux of the order of 0.1 which can also be considered reasonably consistent with the predictable non-zero modulations.

In figure 4, one can see how, for an array of four junctions, the modulation with different periods changes. One can see that, next to the main maximum at zero field, there are two small secondary maxima with two shorter modulation periods. The curve through the data shows again the fit to equation (3). For figure 4(a), the distance between the junctions is 5 μm, while for figure 4(b) is 10 μm. We can conclude that equation (3) provides a good explanation for grid-arrays for both odd and even number of junctions. The fact that in some cases we present only the positive field axis of the patterns is because we collected a large amount of data from measurements on several samples and, in order to maximize the collected information, we often just checked the symmetry of maxima and minima of the patterns for positive and negative values of the magnetic field, but measured the current modulations only for one direction of the field.

We turn now to the analysis of the dynamical features of our system. The external magnetic field applied to the arrays in the plane of the junctions generates Fiske steps (FS) in
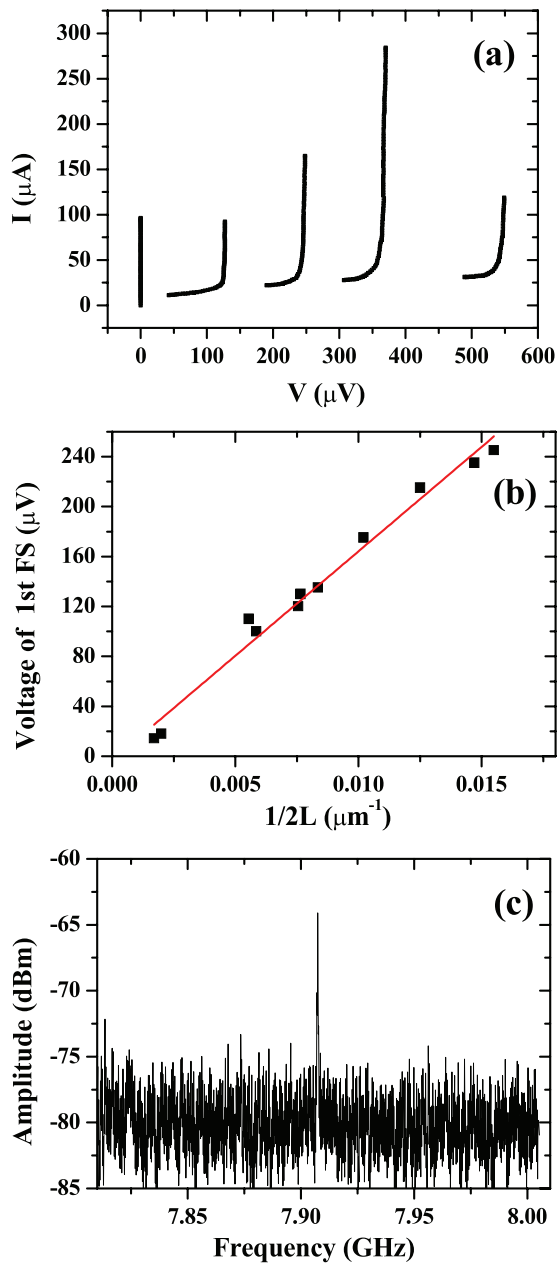
J. Phys. D: Appl. Phys. 49 (2016) 065303

M Lucci *et al*

Figure 5. (a) The current-voltage characteristics of a four-junction interferometer showing Fiske steps; (b) The dependence of the voltage of the 1st Fiske step upon the inverse of the physical length of the arrays showing that the resonances take place over the whole length of the array. The straight through the data represents a linear fit; (c) the radiation emitted when biased at about 16 μV on the Fiske step of a 600 μm long junction.

the current-voltage characteristic, see an example is given in figure 5(a) for an array of four junctions of total length of $L = 66$ μm. These steps were observed at voltages $V_{nFS} = \Phi_0\left(\frac{n\bar{c}}{2L}\right)$, where $\bar{c} = 0.028\,c$ is the speed of light in the transmission line containing the junctions (c is the speed of light in vacuum) and n an integer. Bearing in mind that the capacitance per unit length of our transmission lines is mainly determined by the contribution of the junctions, from this value of the speed of light in the transmission line, assuming the relative permittivity of Al$_2$O$_3$ values in the interval (30–70)

fF μm^{-2}, we have estimated that the thickness of our dielectric barrier is in the range (1–2) nm.

The existence of the Fiske steps reflects dynamical features of our samples. The voltage of the 1st Fiske step (and the voltage spacing between following steps) is $\Phi_0\left(\frac{\bar{c}}{2L}\right)$. In order to check the validity of the model we have plotted (see figure 5(b)) the voltage of the 1st Fiske step of all the arrays that we have tested as a function of the ratio $\left(\frac{1}{2L}\right)$. One can see that the dependence is very close to linear and the straight line fitting the data has a slope $(1.67 \pm 0.08) \times 10^{-8}$ V m, which is consistent with the expected $\Phi_0\bar{c} = 1.73 \times 10^{-8} = 1.73 \times 10^{-8}$ V m value. Thus, the positions of the steps, given the specific light propagation velocity in the discrete line, can be calculated just as done for a continuous junction of the same physical length. This is particularly surprising if we think that the junctions are spaced here by distance up to 30 μm, which is less than the Josephson penetration depth λ_j of the array, but still represents a relatively wide extension for a discontinuity. In figure 5(c), we show a spectrum of emitted Josephson radiation measured at 7.91 GHz when biasing at about 16 μV on the first Fiske step of a 600 μm long array made of 50 junctions having an area of (9 μm × 9 μm) and spaced 2 μm. The radiation could be detected here due to the availability of a receiver in the (6–18) GHz range [7].

We have also measured the modulation of the current amplitudes of the Fiske steps and examples are shown in figure 6. In this figure, we report the measurements of a 34 μm long three-junction interferometer made of junctions having an area of (9 μm × 9 μm) and spaced 2 μm. Figure 6(a) shows the modulation of the maximum Josephson current of this sample fitted to equation (3). Figures 6(b) and (c) show the maximum current modulations of the first (b) and second (c) Fiske steps of this sample, respectively. The 1st and 2nd Fiske steps appeared in this case at voltages of 235 μV and 470 μV, which correspond to the Josephson radiation at 114 and 227 GHz. The normalized length of this sample L/λ_j in this case was of the order of unity, however, we speculate that in this case it might be more relevant for the dynamics the ratio L/λ_{jeff} which is more safely below unity and determines the fact that we did not observe zero-field steps [1, 11] in this case. We found that increasing the normalized length of the arrays, the Fiske resonances display more complex modulation patterns.

For the case of two intermediate-length junctions connected by a superconductive loop at the boundary, modulations of Fiske steps currents due to the flux through a coupling inductor were reported [15] for a normalized Josephson flux through the coupling inductance of the order of unity, however, the physical configuration was substantially different than that of the present experiment. Here we have Fiske modes generated by oscillations all over a discrete Josephson transmission line while in [14] the Fiske steps were those generated by internal spatial oscillations in the individual junctions which were coupled at one end. Over all, Fiske steps in spatially extended Josephson structures have shown a robust identity even when the junctions were investigated in bias configurations including the interactions with external em
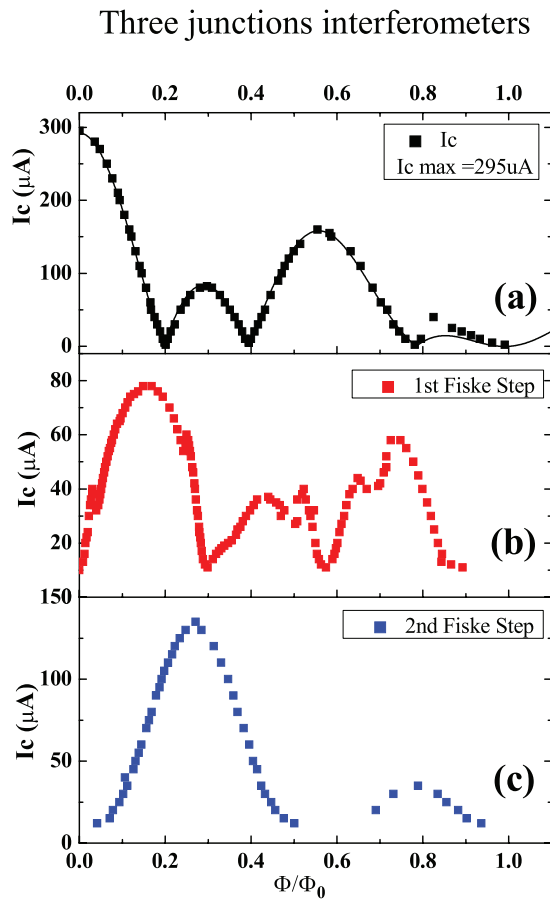
J. Phys. D: Appl. Phys. **49** (2016) 065303

M Lucci *et al*

Three junctions interferometers

Figure 6. (a), (b) and (c) (respectively) maximum Josephson current and the 1st and 2nd Fiske step modulations as a function of the external magnetic field. One can clearly see that the 1st Fiske oscillates out of phase with the Josephson current while the 2nd step modulates in phase with the Josephson current. The curve through the data in (a) is a fit to equation (3).

radiation [16]. A theoretical model (sided by numerical simulations) which could explain the current modulations of Fiske steps in the Josephson structure herein investigated could be an extension of the work performed by Paternò *et al* [17] for low-inductance two-junction interferometers.

As far as 1D arrays of junctions are concerned results for modulations of Josephson currents and evidences of resonances (typically for grids made of 10 junctions or more) were reported [18, 19] but in the literature we haven't found a systematic investigation of stability, radiation emission, and current modulations of the Fiske steps. In the cases of [18] and [19] the normalized Josephson current flux through the connecting inductors ($l_0 I_{C0}/\Phi_0$) was in the range (0.016–0.2), however the physical structure of the arrays was substantially different from ours.

The information that we extract from figures 5 and 6 is that, in spite of the discreteness of the transmission line embedding the Josephson junctions, very stable spatial oscillations of the phase occur over the whole length of the transmission line. This can be either an interesting advantage (or a problem) to consider, depending on possible applied aspect counterpart, however, a similar physical result had been also found by other authors in a similar context in which the analysis of

a Josephson lines with discontinuities was performed [20]. An advantage is represented, for example, by the fact that coupling an external magnetic field to the discrete JTL is eased by the larger areas of the superconducting loops connecting the junctions. A disadvantage, as far as oscillations are concerned, can be the fact that complex and/or unknown internal modes develop inside the discrete structure due to the underdamped nature of the junctions. It is worth noting that applications for new computational concepts [4–6] generally require, for space compactness of the devices, junctions of smaller areas (few micron squares) meaning that critical current densities substantially higher than ours (at least one order of magnitude) are chosen in order to have values of Josephson currents reasonable for practical devices. We believe that these two conditions could lead to characteristics of the devices which are not far from what we measured on our samples. In any case, scaling down the dimension of the arrays shall be an interesting project to pursue.

In conclusion, we have reported experimental results on static and dynamic interference patterns in underdamped arrays of Josephson junctions. We have shown that the experimental results are consistent with the theoretical model, which is linking together, for the physical case of interest, the modulation of the supercurrent of the arrays (due to the superconductive loops connecting the junctions) and the modulation due to the flux threading the junctions. The equation provided by the theoretical model for the maximum Josephson current modulation of a 1D array is analogous to the law predicting the modulations of the intensity of a 1D grid. Therefore, our work demonstrates once more the versatility of Josephson effect and superconducting wave functions to model wave phenomena observed under other physical circumstances. In spite of the fact that the junctions of the array represent relevant discontinuities in the capacitance of the JTL, the presence of stable Fiske modes (and their current modulations) in the current-voltage characteristics demonstrates that stable and coherent phase oscillations take place over the whole length of the array. Considering that stable Fiske modes were observed for voltages all over the wide range (0.1–0.7) mV, we speculate that an adequate integrated planar wave guides design for our samples could lead to highly monochromatic sources (notice the low dynamical resistance of the steps of figure 5(a) and the narrow emission peak in figure 5(c)) of electromagnetic radiation in the (sub-)terahertz range that to be coupled to various other devices or loads.

References

[1] Ustinov A V, Cirillo M, Larsen B H, Oboznov V A, Carelli P and Rotoli G 1995 *Phys. Rev.* **B51** 3081

J. Phys. D: Appl. Phys. 49 (2016) 065303

M Lucci *et al*

van der Zant H S J, Orlando T P, Watanabe S and Strogatz S H 1995 *Phys. Rev. Lett.* **74** 174

[2] Trías E, Mazo J J and Orlando T P 2000 *Phys. Rev. Lett.* **84** 741
Binder P, Caputo P, Fistul M V, Ustinov A V and Filatrella G 2000 *Phys. Rev.* B **62** 8679

[3] Tinkham M 1996 *Introduction to Superconductivity* 2nd edn (New York: Dover) sect. 6.6

[4] Semenov V K, Danilov G V and Averin D V 2003 *IEEE Trans. Appl. Supercond.* **13** 938
Ren J and Semenov V K 2011 *IEEE Trans. Appl. Supercond.* **21** 780

[5] Mukhanov O A 2011 *IEEE Trans. Appl. Supercond.* **21** 760
Volkmann A *et al* 2013 *Supercond. Sci Technol.* **26** 015002

[6] Herr Q P, Herr A Y, Oberg O T and Ioannidis A G 2011 *J. Appl. Phys.* **109** 103903
Oberg O T, Herr Q P, Ioannidis A G and Herr A 2011 *IEEE Trans. Appl. Supercond.* **21** 571

[7] Lucci M, Badoni D, Merlo V, Ottaviani I, Salina G, Cirillo M, Ustinov A V and Winkler D 2015 *Phys. Rev. Lett.* **115** 107002

[8] De Luca R, Di Matteo T, Tuohimaa A and Paasi J 1998 *Phys. Lett.* **245A** 301

[9] Miller J H, Gunaratne G H, Huang J and Golding T D 1991 *Appl. Phys. Lett.* **59** 3330

[10] Gurwitch M, Washington W A and Huggins H A 1983 *Appl. Phys. Lett.* **42** 472

[11] Barone A and Paternò G 1982 *Physics and Applications of the Josephson Effect* (New York:Wiley) see in particular chapt. 12 (eq. 12.3.10)

[12] Caputo J G and Loukitch L 2005 *Physica* **425** 68
Caputo J G and Loukitch L 2007 Collection "Special Topics" of *Eur. J. Phys.* **147** 95–112

[13] Born M and Wolf E 1991 *Principles of Optics* 6th edn (Oxford: Pergamon) sect. 8.6.1

[14] Franz A, Wallraff A and Ustinov A V 2001 *J. Appl. Phys.* **89** 471
Caputo J G, Flytzanis N and Vavalis E 1996 *Int. J. Mod. Phys.* C **7** 191

[15] Cirillo M, Pace S, Pagano S and Paternò G 1985 *Phys. Lett.* **109A** 117
Cirillo M 1985 *J. Appl. Phys.* **58** 3217

[16] Grønbech-Jensen N and Cirillo M 1994 *Phys. Rev.* **B50** 12851

[17] Paternò G, Cucolo A M and Vaglio R 1986 *J. Appl. Phys.* **60** 1455

[18] Cirillo M, Larsen B H, Ustinov A V, Merlo V, Oboznov V A and Leoni R 1993 *Phys. Lett.* A **183** 383–9

[19] Gambardella U, Caputo P, Boffa V, Celentano G, Costabile G and Pace S 1996 *J. Appl. Phys.* **79** 322

[20] Nappi C, Sarnelli E, Adamo M and Navacerrada P A 2006 *Phys. Rev.* **B74** 144504 see in particular the arguments leading to eq. 26